8748 *Biochemistry* **2010,** *49,* 8748–8755
DOI: 10.1021/bi100817q

BIOCHEMISTRY
including biophysical chemistry & molecular biology
*Article*

# Archaeal RibL: A New FAD Synthetase That Is Air Sensitive†

Zahra Mashhadi, Huimin Xu, Laura L. Grochowski, and Robert H. White*

*Department of Biochemistry (0308), Virginia Polytechnic Institute and State University, Blacksburg, Virginia 24061*

*Received May 21, 2010; Revised Manuscript Received September 6, 2010*

ABSTRACT: FAD synthetases catalyze the transfer of the AMP portion of ATP to FMN to produce FAD and pyrophosphate ($PP_i$). Monofunctional FAD synthetases exist in eukaryotes, while bacteria have bifunctional enzymes that catalyze both the phosphorylation of riboflavin and adenylation of FMN to produce FAD. Analyses of archaeal genomes did not reveal the presence of genes encoding either group, yet the archaea contain FAD. Our recent identification of a CTP-dependent archaeal riboflavin kinase strongly indicated the presence of a monofunctional FAD synthetase. Here we report the identification and characterization of an archaeal FAD synthetase. *Methanocaldococcus jannaschii* gene MJ1179 encodes a protein that is classified in the nucleotidyl transferase protein family and was previously annotated as glycerol-3-phosphate cytidylyltransferase (GCT). The MJ1179 gene was cloned and its protein product heterologously expressed in *Escherichia coli*. The resulting enzyme catalyzes the adenylation of FMN with ATP to produce FAD and $PP_i$. The MJ1179-derived protein has been designated RibL to indicate that it follows the riboflavin kinase (RibK) step in the archaeal FAD biosynthetic pathway. Aerobically isolated RibL is active only under reducing conditions. RibL was found to require divalent metals for activity, the best activity being observed with $Co^{2+}$, where the activity was 4 times greater than that with $Mg^{2+}$. Alkylation of the two conserved cysteines in the C-terminus of the protein resulted in complete inactivation. RibL was also found to catalyze cytidylation of FMN with CTP, making the modified FAD, flavin cytidine dinucleotide (FCD). Unlike other FAD synthetases, RibL does not catalyze the reverse reaction to produce FMN and ATP from FAD and $PP_i$. Also in contrast to other FAD synthetases, $PP_i$ inhibits the activity of RibL.

Riboflavin (vitamin $B_2$) is the redox-active component of FMN and FAD, which are essential coenzymes in all free-living organisms. Phosphorylation of riboflavin to FMN and subsequent adenylation of FMN[1] to FAD are catalyzed by the enzymes riboflavin kinase and FAD synthetase, respectively. It is known that bacteria have a bifunctional enzyme that catalyzes both the phosphorylation and the adenylation reactions to convert riboflavin to FAD (*1*, *2*). The kinase active site is located in the C-terminus, and the adenylyltransferase active site is located in the N-terminus of the bifunctional *Escherichia coli* enzyme, RibF (*3*, *4*). Eukaryotes have two separate monofunctional enzymes each catalyzing one of the reactions (*5*).

The Archaeal riboflavin biosynthetic pathway exhibits many differences from the canonical pathway, in terms of both the genes encoding the enzymes for the pathway and the pathway itself (*6*−*9*). One of the differences is that archaeal genomes do not contain homologues of canonical riboflavin kinase and FAD synthetase. Although all known nonarchaeal riboflavin kinases use ATP as a phosphoryl donor, archaea contain a monofunctional enzyme, RibK, that phosphorylates riboflavin with CTP (*6*). Here we report the identification and characterization of the archaeal monofunctional FAD synthetase from *Methanocaldococcus jannaschii*, now designated RibL, which is encoded by the MJ1179 gene. The MJ1179-encoded protein is classified as a nucleotidyl transferase and was previously annotated as glycerol-3-phosphate cytidylyltransferase (GCT) (www.ncbi.nlm.nih.gov). Aligning the RibL sequence with its homologues shows the existence of two conserved cysteines at the C-terminal part of these proteins. The involvement of these cysteines in catalytic activity of RibL was also investigated.

## MATERIALS AND METHODS

*Chemicals*. All chemicals were obtained from Sigma/Aldrich.

*Identification of FAD in M. jannaschii by LC*−*ES-MS*. Frozen *M. jannaschii* cells (*10*) (∼50 mg wet weight) were suspended in 200 μL of extraction buffer {50 mM *N*-[tris(hydroxymethyl)methyl]-2-aminoethanesulfonic acid (TES) (pH 7.0), 10 mM $MgCl_2$, and 20 mM DTT} and lysed by sonication. All *M. jannaschii* proteins in the extracted sample (40 mg/mL) were denatured and precipitated via addition of 20 μL of 2 M trichloroacetic acid (TCA). After centrifugation (16000*g* for 10 min), the pellet was suspended in 50 μL of water and recentrifuged, and the supernatant was combined with the first soluble fraction. The soluble fraction was washed three times with 100 μL of diethyl ether to remove all of the TCA, producing an extract with a pH of ∼6.5.

LC−ES-MS was used to separate and identify FAD in the prepared extract. An Agilent HPLC system equipped with a

†This work was supported by National Science Foundation Grant MCB 0722787 to R.H.W.

*To whom correspondence should be addressed. Telephone: (540) 231-6605. Fax: (540) 231-9070. E-mail: rhwhite@vt.edu.

[1]Abbreviations: GTP, guanosine 5′-triphosphate; CTP, cytidine 5′-triphosphate; DTT, dithiothreitol; TES, *N*-tris(hydroxymethyl)methyl-2-aminoethanesulfonic acid; ICPES, inductively coupled plasma emission spectrophotometry; HEPES, *N*-(2-hydroxyethyl)piperazine-*N*-2-ethanesulfonic acid; FMN, flavin mononucleotide; FAD, flavin adenine dinucleotide, $PP_i$, pyrophosphate; FCD, flavin cytidine dinucleotide; GCT, glycerol-3-phosphate cytidylyltransferase; LC−ES-MS, liquid chromatography−electrospray mass spectroscopy; TFAA, trifluoroacetic anhydride; TLC, thin-layer chromatography; IAA, iodoacetamide; ME, β-mercaptoethanol.

 Published on Web 09/07/2010 

ZORBAX Eclipse XDB-C18 column (4.6 mm inside diameter × 50 mm length, 1.8 μm particle size) was used for separation of *M. jannaschii* cell extract components. This HPLC system was interfaced with a 3200 Q TRAP mass spectrometer. The elution profile consisted of a linear gradient from 95% ammonium acetate solution (25 mM) and 5% methanol to 35% ammonium acetate solution (25 mM) and 65% methanol over 10 min at a rate of 0.5 mL/min. Under these chromatographic conditions, FAD eluted at 7.7 min.

*Cloning and Recombinant Expression of RibL and Its Mutants*. The MJ1179 gene that encodes the protein identified by Swiss-Prot accession number Q58579 (*11*) was amplified by polymerase chain reaction (PCR) from genomic DNA (*12*) using oligonuculeotide primers MJ1179Fwd (5′-GGTCATATGAAA-AAGAGGGTAG-3′) and MJ1179Rev (5′-GCTGGATCCT-TAGATTTTAATCTC-3′). Purified PCR product was digested with *Nde*I and *Bam*HI restriction enzymes. DNA fragments were ligated into compatible sites in plasmid pT7-7 to generate pMJ1179. Two mutations of MJ1179, C126S and C143S, were generated using the QuikChange site-directed mutagenesis kit using pMJ1179 as a template. The C126S primers were 5′-GGT-TATAAAAAAAGTCCATTTCACAG-3′ (forward) and 5′-CTGT-GAAATGGACTTTTTTTATAAC-3′ (reverse). The C143S primers were 5′-GGAGATTCAGCAATAAAGAG-3′ (forward) and 5′-CTCTTTATTGCTGAATCTC-3′ (reverse). The mutations were confirmed by sequencing of their plasmid inserts (pMJ1179 C126S and pMJ1179 C143S). Recombinant plasmids, either pMJ1179 or one of the mutated plasmids, were transformed into *E. coli* strain BL21-Codon Plus (DE3)-RIL. RibL and its mutants were expressed as described previously (*12*). Induction of RibL and its mutants was confirmed by sodium dodecyl sulfate−polyacrylamide gel electrophoresis (SDS−PAGE).

*Purification of Recombinant RibL and Its Mutants*. A frozen *E. coli* cell pellet (~0.4 g wet weight from 200 mL of medium) was suspended in 3 mL of extraction buffer and lysed by sonication. The samples were then centrifuged (16000*g* for 10 min) to remove cell debris, and the resulting cell extract was heated for 10 min at 70 °C followed by centrifugation (16000*g* for 10 min). This process allowed for the purification of RibL or its mutants from the majority of *E. coli* proteins, which denature and precipitate under these conditions. The next step of purification was performed by anion-exchange chromatography of the 70 °C soluble fractions on a MonoQ HR column (1 cm × 8 cm; Amersham Bioscience) using a linear gradient from 0 to 1 M NaCl in 25 mM TES buffer (pH 7.5), over 55 min at a flow rate of 1 mL/min, and collecting 1 mL fractions. Protein concentrations were determined by Bradford analysis (*13*).

*Metal Ion Analysis of RibL and Its Mutants*. Metal analysis of purified RibL was performed at the Virginia Tech Soil Testing Laboratory using inductively coupled plasma emission spectrophotometry (ICPES). The MonoQ purified proteins were diluted in 25 mM Tris buffer (pH 7.5) to give a final calculated metal concentration of 0.05 ppm prior to analysis, assuming 1 equiv of metal per protomer. Samples were analyzed for iron, manganese, magnesium, zinc, and cobalt. The detection limits for these metals were 0.008, 0.002, 0.05, 0.005, and 0.008 mg/L, respectively.

*Measurement of the Native Molecular Mass of RibL*. The native molecular mass of RibL was determined by size exclusion chromatography on a Superose 12HR column (10 mm × 300 mm) developed with buffer containing 50 mM HEPES (pH 7.2) and 150 mM NaCl at rate of 0.5 mL/min with detection at 280 nm. Protein standards used to calibrate the column included apoferritin (443 kDa), alcohol dehydrogenase (150 kDa), conalbumin (77 kDa), and vitamin $B_{12}$ (1.4 kDa).

*Analysis of the Enzymatic Activity of RibL and Its Mutants*. The standard assay for RibL was performed by incubation of 2 μg of RibL in 35 mM TES ($K^+$) buffer (pH 7.2) containing 14 mM DTT, 7 mM $MgCl_2$, 5.7 mM ATP, and 0.17 mM FMN in a total volume of 35 μL at 70 °C for 15 min. The activity of the mutants was tested with 3.5 μg of RibLC126S or 5.5 μg of RibLC143S under the standard assay conditions. As a control, the same MonoQ fraction from *E. coli* cells expressing another gene (MJ0309) was tested for activity under the same conditions. Following incubation, 70 μL of methanol was added to stop the reactions. After centrifugation (16000*g* for 10 min), samples were separated from the pellet and the methanol was removed by evaporation. Water was added to the supernatants to adjust the volumes to 100 μL for HPLC analysis. A Shimadzu HPLC system equipped with an RF-10AXL fluorescence detector and a C18 reverse-phase column (Varian PursuitXRs, 250 mm × 4.6 mm, 5 μm particle size) was used. The elution consisted of 95% sodium acetate buffer (25 mM, pH 6.0, 0.02% $NaN_3$) and 5% methanol for 5 min followed by a linear gradient to 20% sodium acetate buffer and 80% methanol over 40 min at a rate of 0.5 mL/min. Under these conditions, flavins were eluted in the following order: FAD at 26.5 min, FMN at 29.0 min, and riboflavin at 31.0 min. Flavins were detected by fluorescence using a $\lambda_{ex}$ of 450 nm and a $\lambda_{em}$ of 520 nm (*6*). A sample at a known concentration of FAD was used to calculate the conversion factor of fluorescent units to nanomoles of FAD. This conversion factor was used to determine the amount of FAD produced in our experiments.

*Testing Alternative Substrates*. RibL was tested for its ability to use other nucleotides such as CTP and GTP to transfer CMP and GMP to FMN to produce the modified FADs, flavin cytosine dinucleotide (FCD), and flavin guanine dinucleotide (FGD). The standard assay conditions were used in the incubation in the presence of 2 μg of RibL, 0.084 mM FMN, and either 5.7 mM CTP or GTP instead of ATP. To test if RibL would catalyze the production of CDP-glycerol from glycerol 3-phosphate and CTP, the enzyme was incubated with 10 mM CTP, 17 mM DL-glycerol 3-phosphate, and 2.8 mM $MgCl_2$ under the standard assay conditions. The production of the products was assessed using the MonoQ protein separation procedure described above. This method allowed the separation and quantitation of CMP, CDP, and CTP, which eluted at 0.21, 0.29, and 0.35 M NaCl, respectively.

*Metal Ion Dependency of the RibL Reaction*. The assay for the metal dependency of RibL was performed by incubation of 2 μg of RibL with 5.7 mM ATP, 0.084 mM FMN, and 2.8 mM $MgCl_2$, $MnCl_2$, $ZnCl_2$, $CoCl_2$, $NiCl_2$, or $Fe(NH_4)_2(SO_4)_2$ or no metal under the standard assay conditions. In the case of $Fe(NH_4)_2(SO_4)_2$, argon gas was used to remove oxygen and prevent oxidation of the Fe(II) in the sample vial.

*Synthesis of Flavin Cytidine Dinucleotide* (*FCD*). We synthesized FCD by dissolving 0.1 g of FMN and 35 mg of CMP in 1 mL of trifluoroacetic anhydride (TFAA). The procedure was based on the previously described preparation of FAD from FMN and AMP (*14*). After the reactants dissolved (~1 min), the sample was kept in the dark for 18 h. Following incubation, a stream of $N_2$ gas was used to evaporate the solvent. The recovered dried yellow powder was dissolved in water and purified by preparative thin-layer chromatography (TLC) using

a solvent system consisting of 0.2 M ammonium bicarbonate in acetonitrile, water, and formic acid (80:20:10, v/v/v). The flavin-containing compounds were visualized as yellow spots that were fluorescent upon exposure of the TLC plates to UV light. The identification of recovered FCD was established by its absorbance spectra and ES-MS analysis by direct infusion of the solution in ammonium acetate (1 g/L) buffer.

*Preparation and Characterization of the Enzymatically Prepared FCD and FAD*. RibL (4 $\mu$g) was incubated in 28 mM TES ($K^+$) buffer (pH 7.2) containing 5.7 mM $MgCl_2$, 0.9 mM FMN, and either 14 mM CTP or ATP in a total volume of 30 $\mu$L at 70 °C for 45 min. Separation of the product and substrates was performed by preparative TLC as described above. Under these conditions, the retention factor ($R_f$) values for ATP, CTP, FMN, FAD, and FCD were 0.0, 0.0, 0.3, 0.15, and 0.18, respectively. The yellow FAD and FCD bands were eluted from the silica plate with water and dissolved in 100 $\mu$L of ammonium acetate (1 g/L) buffer for ES-MS by direct infusion.

*Identification of the Enzymatic Reaction Product as Pyrophosphate*. The $PP_i$ produced by the enzymatic reaction was assayed by enzymatic coupling to the oxidation of NADH utilizing pyrophosphate-dependent fructose-6-phosphate kinase, fructose-1,6-diphosphate aldolase, triose phosphate isomerase, and α-glycerophosphate dehydrogenase provided by the pyrophosphate reagent product from Sigma (P7275). The incubation mixtures consisted of 29 mM TES (pH 7.5), 1.8 mM $CoCl_2$, 0.4 mM FMN, 4.5 mM ATP, and 12 $\mu$g of RibL in a total volume of 110 $\mu$L. The control mixture was the same as the sample mixture but without FMN. Following incubation at 70 °C for 30 min, sample mixtures were cooled on ice, centrifuged, and combined with 100 $\mu$L of pyrophosphate reagent at 30 °C in a 100 $\mu$L cuvette. The oxidation of NADH was monitored at 340 nm.

*Determination of the Kinetic Parameters*. Assays for determining the kinetic constants for ATP were performed under the standard assay conditions with the following modifications. In this assay, 2 $\mu$g of RibL was incubated in 35 mM TES ($K^+$) buffer (pH 7.2), 7 mM $MgCl_2$, and 0.17 mM FMN in the presence of either 0, 0.014, 0.03, 0.06, 0.2, 0.3, 0.6, 1.4, 2.8, or 5.7 mM ATP or CTP in a total volume of 35 $\mu$L at 70 °C for 15 min. To determine the kinetic constants for FMN, we performed the assay as described above in the presence of 5.7 mM ATP and the concentration of FMN was varied (0, 5, 10.5, 21, 42, or 84 $\mu$M).

Assays to determine the mechanism of the reaction catalyzed by RibL were performed under the standard assay conditions with the following modifications. In these assays, 2 $\mu$g of RibL was incubated in 35 mM TES ($K^+$) buffer (pH 7.2) and 7 mM $MgCl_2$ in the presence of different concentrations of FMN (5, 21, 50, and 84 $\mu$M) and ATP (0.057, 0.29, 0.57, and 1.4 mM) in a total volume of 35 $\mu$L at 70 °C for 15 min.

*Inhibition of the RibL Reaction by Pyrophosphate and the Reversibility of the Reaction*. The assay was performed under the standard assay conditions with different concentrations of $PP_i$ (0.28, 1.4, and 7.1 mM) being added to the reaction mixture. To see if RibL would catalyze the reverse reaction, 0.4 mM FAD and 5 mM $PP_i$ were incubated under the standard assay conditions and the formation of FMN was measured. HPLC was used to analyze the product.

*Testing the Effects of the Redox State of RibL on Its Activity*. Two sets of experiments were conducted to examine the role of the two conserved cysteines at the C-terminal end of RibL. In the first experiment, 2 $\mu$g of RibL was incubated in 37.5 mM TES ($K^+$) buffer (pH 7.2), 5.6 mM DTT, and 0.1 mM FMN in a total volume of 32 $\mu$L at room temperature for 15 min under argon gas. ATP (5 mM) and either $MnCl_2$ or $Fe(NH_4)_2(SO_4)_2$ at a total concentration of 2.5 mM were added. Samples were incubated at 70 °C for 15 min and then assayed for FAD by HPLC. A control mixture contained the same components but without DTT in the presence of $MnCl_2$. In the second experiment, cysteines were alkylated to see if this affected the activity of RibL. The samples that contained 2 $\mu$g of RibL in 37.5 mM TES ($K^+$) buffer (pH 7.2) and 4 mM DTT in a total volume of 11 $\mu$L were incubated at room temperature for 15 min. Argon gas was used to remove the oxygen from the incubating mixture. Iodoacetamide (IAA) at a final concentration of 11.8 mM was added to the sample followed by a 25 min incubation at room temperature followed by addition of β-mercaptoethanol (ME) at a final concentration of 48 mM to remove excess IAA. ATP (5.7 mM), 0.1 mM FMN, and $MnCl_2$ at a total concentration of 2.9 mM were added. The sample in a total volume of 35 $\mu$L was incubated at 70 °C for 15 min and then assayed for FAD by HPLC.

## RESULTS

*Identification of FAD in M. jannaschii*. The existence of FAD in *M. jannaschii* was investigated and confirmed. The HPLC eluted FAD peak was identified based on its fluorescence, absorbance, and MS/MS spectra.

*Expression and Purification of RibL and Its Mutants*. The MJ1179 gene from *M. jannaschii* and its C126S and C143S mutants were cloned and overexpressed in *E. coli*. The recombinantly expressed proteins were extracted from the cells by sonication and purified by heating the extracts at 70 °C for 10 min followed by anion-exchange chromatography. SDS−PAGE analysis of the purified RibL and the mutants with Coomassie staining showed a single band corresponding to a molecular mass of ~17 kDa with a purity of >95%. This molecular mass is consistent with the predicted monomeric molecular mass of 17288 Da for RibL. Approximately the same amount of each protein was isolated, indicating that the mutations did not reduce the protein's heat stability or solubility. Size exclusion chromatography yielded a molecular mass of 29 kDa, consistent with the RibL existing as a dimer.

*Identification of the Reaction Catalyzed by RibL*. Incubation of RibL with FMN and ATP at 70 °C for 15 min produced a new fluorescent compound when the reaction mixture was assayed either by HPLC using fluorescence detection at the flavin excitation and emission wavelengths or by TLC. The peak was identified as FAD on the basis of its HPLC elution time (26.5 min) and TLC ($R_f$ = 0.15) as compared to those of a known. The new peak had the FAD absorbance spectrum, which had $\lambda_{max}$ values at 266, 371, and 450 nm. LC−MS of the TLC-purified product gave the same ES-MS spectrum as an authentic sample of FAD showing an $[M - H]^-$ ion at $m/z$ 784.4. The Ar collisionally induced fragmentation of the ion at $m/z$ 784.4 for both known and enzymatically generated FAD gave the same set of fragment ions at $m/z$ 517.1, 455.3, 437.3, 408.3, and 346.3.

To determine if the other product(s) of this reaction was one pyrophosphate or consisted of two inorganic phosphates, the $PP_i$ generated in the reaction mixture was assayed. This assay revealed that $PP_i$ is the other product of adenylation of FMN by RibL. An incubation containing 0.4 mM FMN produced

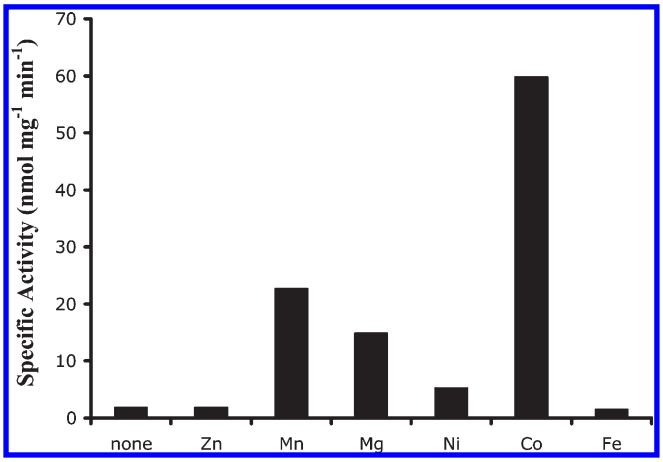


FIGURE 1: Dependency of divalent metals on the RibL-catalyzed conversion of ATP and FMN to FAD and $PP_i$. MonoQ-purified RibL (2 $\mu$g) was incubated with 5.7 mM ATP, 0.084 mM FMN, and either no added metal or the indicated metals at 2.8 mM in the presence of 14 mM DTT in a total volume of 35 $\mu$L of TES buffer. Only the Fe(II) assay was conducted under argon gas.

0.10 mM $PP_i$ and 0.10 mM FAD, indicating that no phosphate was generated in the incubation.

*Substrate Specificity of the RibL Reaction*. RibL was able to utilize other nucleotides such as CTP and GTP as substrates, producing the modified coenzymes, FCD and FGD, respectively. The FCD product was confirmed by comparison to a known, synthetically prepared sample. The specific activity of RibL with ATP, CTP, or GTP as the nucleotidyl donor was measured under standard assay conditions with 0.084 mM FMN and either ATP, CTP, or GTP (5.7 mM). The specific activity of RibL is 10, 4, and 1 nmol mg$^{-1}$ min$^{-1}$ with ATP, CTP, and GTP, respectively. LC−MS of the TLC-purified FCD produced in the CTP incubation gave the same ES-MS spectrum as an authentic sample showing an $[M - H]^-$ ion at $m/z$ 760.2. The Ar collisionally induced fragmentation of the ion at $m/z$ 760.2 for both the synthesized and enzymatically generated FCD gave ions at $m/z$ 517.1, 437.2, 384.1, and 322.1. RibL did not function as a glycerol-3-phosphate cytidylyltransferase because it failed to catalyze the formation of glycerol cytidine dinucleotide when incubated with DL-glycerol 3-phosphate and CTP.

*Metal Content and Metal Ion Dependency of the RibL Reaction*. ICPES was used to determine the identity and quantity of metal ions present in the purified recombinant enzyme. RibL was found to contain 0.2 mol of iron and 8.4 mol of magnesium per protomer when the protein concentration was determined by the Bradford protein assay. We suspect that the large ratio of metals per protomer reflects nonspecific binding of magnesium to the protein. Both RibLC126S and RibLC143S were found to contain $<0.8$ and $<0.08$ mol of Mg and Fe per protomer, respectively. Assaying the activity of RibL to form FAD in the presence of different metals revealed that RibL has its best activity in the presence of $Co^{2+}$ (Figure 1) where the activity was 4 times greater than that with $Mg^{2+}$.

*Determination of the Kinetic Parameters*. The specific activity of RibL versus different concentrations of ATP up to 1.4 mM was fit to a hyperbolic curve (Figure 2A) and shows that RibL reaches its maximal activity at an ATP concentration of ~1.4 mM. The RibL activity decreases by 20% when the concentration of ATP is higher than the physiologically relevant concentration (~5 mM). When using CTP as the nucleotidyl donor, the activity of RibL reaches its maximal activity at a CTP concentration of ~1.4 mM (Figure 2B). In this case, the RibL maximal activity decreases by 68 and 95% when the concentration of CTP was 5.7 and 11.4 mM, respectively. The RibL kinetics were determined under steady state conditions in the presence of either 5.7 mM ATP or 0.17 mM FMN as the fixed substrate concentration. KeleidaGraph 4.0 was used to fit the data for ATP and CTP (Figure 2A,B) to the Michaelis−Menten plot with substrate inhibition using the equation $Y = (V_{max}X)/[K_m + X(1 + X/K_i)]$. In the case of FMN as the variable substrate, the data were fitted to a Michaelis−Menten plot. The measured kinetic parameters for RibL with either ATP or CTP as the nucleotidyl donor and FMN as the nucleotidyl acceptor are reported in Table 1. Kinetic parameters for CTP were determined by fitting the data points not showing inhibition to the Michaelis−Menten equation. The later points were omitted because, in this case, the inhibition is dramatic.

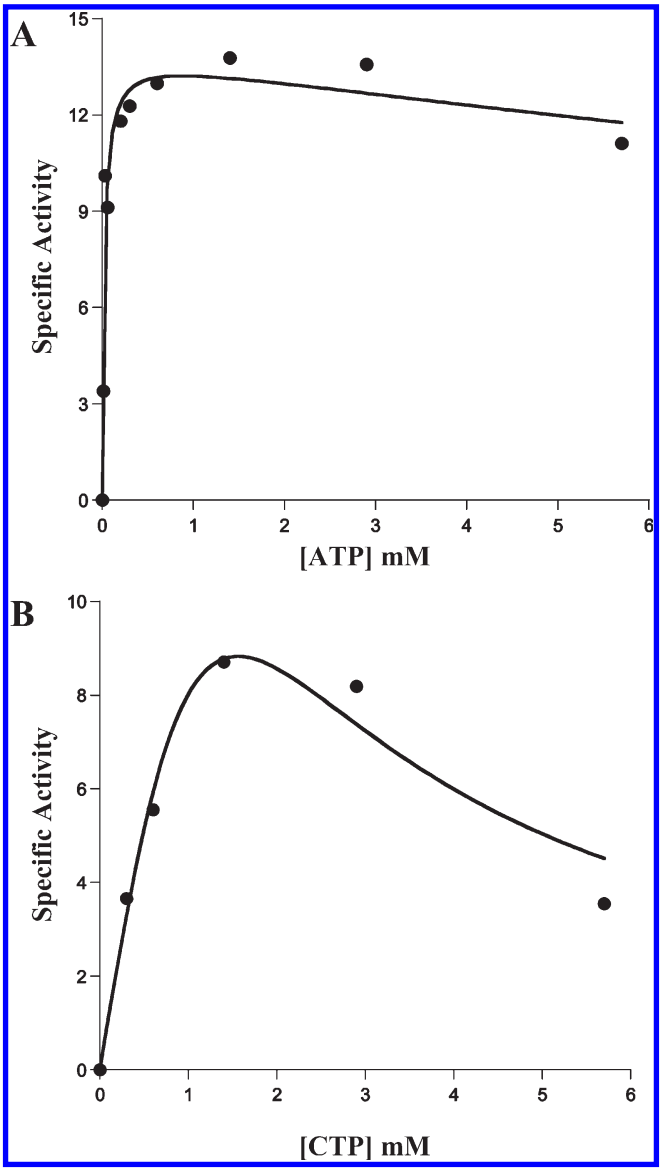


FIGURE 2: Plot of steady state kinetic data for RibL. Measured specific activities (nanomoles per milligram per minute) of RibL at (A) ATP concentrations of 0, 0.014, 0.03, 0.06, 0.2, 0.3, 0.6, 1.4, 2.9, and 5.7 mM and (B) CTP concentrations of 0.0, 0.3, 0.6, 1.4, 2.9, 5.7, and 11.4 mM in the presence of 0.17 mM FMN and 7 mM $Mg^{2+}$. Activities were measured after incubation for 15 min at 70 °C.

The specific activity of RibL was measured in the presence of different concentrations of ATP and FMN up to 1.4 mM and

Table 1: Kinetic Parameters of RibL with Its Substrates[a]

| substrate | $K_M^{app}$ ($\mu$M) | $V_{max}$ (nmol min$^{-1}$ mg$^{-1}$) | $k_{cat}/K_M^{app}$ ($M^{-1}$ $s^{-1}$) | $K_i$ (mM) |
|---|---|---|---|---|
| ATP | 25 ± 7.7 | 14 ± 0.97 | 160 | 31 ± 28 |
| FMN | 63 ± 21 | 14 ± 2.6 | 64 | – |
| CTP | 480 ± 170 | 10 ± 1.1 | 6 | – |

[a]The RibL kinetics was determined under steady state conditions. FMN at concentration of 0.17 mM was used as the fixed substrate to determine the kinetic values for either ATP or CTP as the nucleotidyl donor. The concentrations of ATP and CTP were varied from 0 to 5.7 mM in the presence of 0.17 mM FMN. ATP at a concentration of 5.7 mM was used as the fixed substrate to determine the kinetic values for FMN as the nucleotidyl acceptor. The concentration of FMN was varied from 0 to 84 $\mu$M.

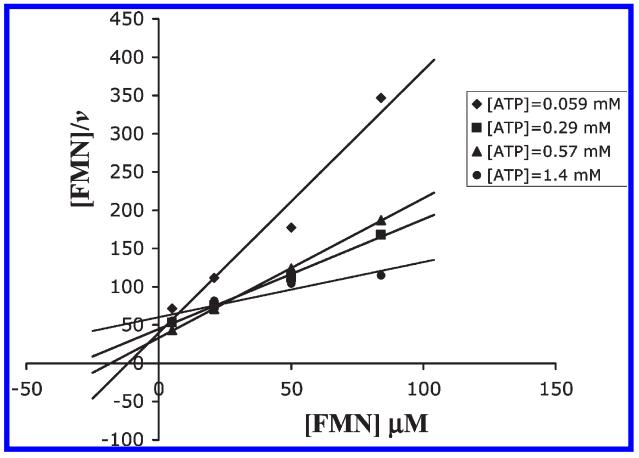


FIGURE 3: Hanes plots of [FMN]/$v$ (milligram per minute per milliliter) vs [FMN] (micromolar) in the presence of different concentrations of ATP. The specific activities (nanomoles per milligram per minute) of RibL were measured in the presence of different concentrations of FMN (5, 21, 50, and 84 $\mu$M) and ATP (0.057, 0.29, 0.57, and 1.4 mM) with 7 mM $Mg^{2+}$ after incubation for 15 min at 70 °C.

84 $\mu$M, respectively. A Hanes plot was generated as [FMN]/$v$ versus [FMN] in the presence of different concentrations of ATP (Figure 3), and it shows a series of nonparallel lines that do not intersect at a common point, indicating that RibL proceeds by a ternary complex mechanism with substrate (ATP) inhibition.

*Inhibition of the RibL Reaction by Pyrophosphate and the Reversibility of the Reaction*. Adenylation of FMN by ATP catalyzed by RibL is inhibited by $PP_i$. The activity of RibL decreased by 30, 85, and 95% when the incubation of RibL with FMN and ATP assay was conducted under standard conditions in the presence of 0.28, 1.4, and 7.1 mM $PP_i$, respectively. Incubation of RibL with FAD and $PP_i$ showed no increase in the amount of FMN in the incubation mixture as measured by HPLC.

*Testing the Effects of the Redox State of RibL on Enzymatic Activity*. Sequence alignment of the homologues of RibL identified a shared motif that contains two conserved cysteines. These cysteines could be involved as a redox sensor by forming a disulfide or be involved in metal binding. To test these ideas, two different sets of experiments were conducted. In the first set of experiments, the specific activity of the enzyme was measured under standard assay conditions in the presence of 2.8 mM $MnCl_2$, and either in the presence of DTT under argon or with DTT under air (Table 2). The specific activity of RibL was the highest (40 nmol mg$^{-1}$ min$^{-1}$) in the presence of DTT under argon and decreased to 22 nmol mg$^{-1}$ min$^{-1}$ when the incubation

Table 2: Effects of the Redox State on the Specific Activity of RibL[a]

| | with DTT and Ar | with DTT in air | without DTT in air | alkylated cysteines, with ME in air |
|---|---|---|---|---|
| specific activity (nmol mg$^{-1}$ min$^{-1}$) | 40 | 22 | 3.3 | 0.26 |

[a]All of these experiments were conducted in the presence of 2 $\mu$g of RibL, 5 mM ATP, 0.1 mM FMN, and 2.5 mM $MnCl_2$. The concentrations of DTT and mercaptoethanol (ME) were 5.6 and 40 mM, respectively.

Table 3: Specific Activities (nanomoles per milligram per minute) of RibL and Its Mutants with Different Metals[a]

| | measured specific activity (nmol mg$^{-1}$ min$^{-1}$) | | |
|---|---|---|---|
| added metal | wild-type RibL | RibLC126S | RibLC143S |
| $Mg^{2+}$ | 5.1 | 12 | 4 |
| $Co^{2+}$ | 60 | 0.64 | 0.24 |

[a]All of these experiments were performed under the standard assay conditions in the presence of DTT and air.

was conducted with DTT in the presence of air. In the absence of DTT, RibL exhibited a specific activity of only 3.3 nmol mg$^{-1}$ min$^{-1}$. As a control, the corresponding MonoQ-purified fraction of *E. coli* cells expressing another gene (MJ0309) was tested and a specific activity of 0.04 nmol mg$^{-1}$ min$^{-1}$ was measured.

In another experiment, the two cysteines were reduced by DTT and alkylated with iodoacetamide. Alkylation of both cysteines was confirmed via electrospray mass spectroscopy (ES-MS). The masses of the alkylated tryptic peptides EIIRRFCNK and CPFHSSFDIVK matched the expected alkylated tryptic peptide masses of 1235.6600 and 1552.6289, respectively. After being treated with IAA, RibL lost almost all of its activity as shown in Table 2.

*Activity of RibL's Mutants*. The activities of the RibLC126S and -C143S mutants were measured under the standard assay conditions. The activity of each mutant was tested in the presence of $Mg^{2+}$ and $Co^{2+}$ (Table 3). This experiment revealed that in the presence of $MgCl_2$, RibLC126S had activity (12 nmol mg$^{-1}$ min$^{-1}$) ~2 times higher than that of the wild type (5.1 nmol mg$^{-1}$ min$^{-1}$). The activity of RibLC143S was approximately that of the wild type (4.0 nmol mg$^{-1}$ min$^{-1}$). The specific activities of RibLC126S and RibLC143S in the presence of $CoCl_2$ were 0.64 and 0.24 nmol min$^{-1}$ mg$^{-1}$, respectively, which is very low compared to the wild-type activity of 60 nmol min$^{-1}$ mg$^{-1}$.

*Analysis of Flavins in E. coli Overexpressing RibL and Its Mutants*. After *ribL* had been overexpressed in *E. coli*, the cell extract was only slightly yellow. However, the *E. coli* cell extracts after overexpression of the mutated *ribL* constructs had a much more intense visible yellow color. Flavins eluted from MonoQ-separated cell extracts were used to measure the amount of riboflavin, FMN, and FAD in these extracts. The flavins in the most intense fraction of either RibL or its mutants were analyzed by HPLC with fluorescent detection of the flavin-containing compounds. The fraction from the *ribL* expression contains ~4.8 $\mu$M riboflavin and 3.3 $\mu$M FMN, and it contains no detectable FAD ( < 0.1 $\mu$M). The concentrations in the fractions from the C126S and C143S mutants were 4.8 $\mu$M FMN and 19.1 $\mu$M FAD, and 6.4 $\mu$M FMN and 21.3 $\mu$M FAD, respectively. No riboflavin was detected in MonoQ-purified fractions from either

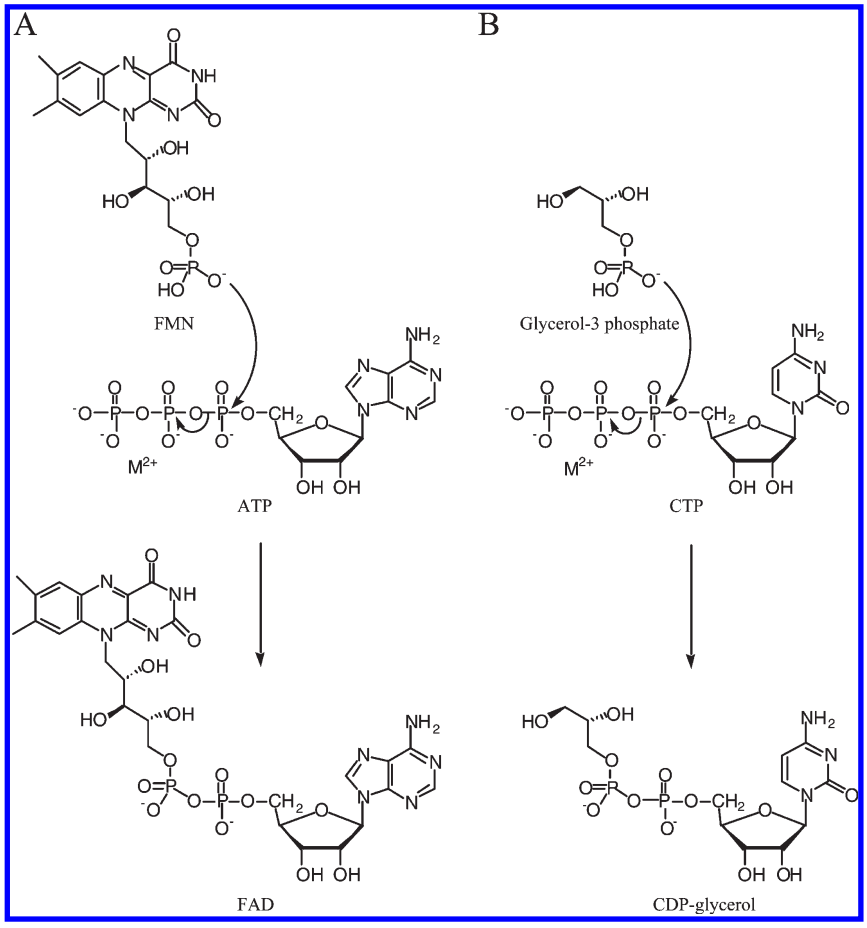


FIGURE 4: Chemical reactions that are catalyzed by (A) FAD synthetase and RibL and (B) GCT. In all cases, the phosphate group of the substrate attacks the α-phosphate of the ATP, resulting in release of inorganic pyrophosphate.

mutant. This indicates that under the in vivo aerobic expression conditions, the cysteine mutants exhibited more activity than the wild-type enzyme.

## DISCUSSION

Until recently, no evidence of the final steps and enzymes involved in the biosynthesis of FAD from riboflavin was apparent in the archaea. This was despite the fact that *M. jannaschii* does contain FAD as indicated by the direct analysis of FAD in the cells, as shown here. Additionally, gene products that have been studied in other organisms known to function with FAD are encoded in the *M. jannaschii* genome. Recently, a new riboflavin kinase was discovered in *M. jannaschii* (RibK) that used CTP as the phosphate donor (*6*, *9*). These observations indicated that a monofunctional FAD synthetase must be present in the archaea. We identified a predicted nucleotidyltransferase, MJ1179, that is annotated as glycerol 3-phosphate cytidylyltransferase (GCT). The product of the reaction catalyzed by GCTs, CDP-glycerol, is a key intermediate in teichoic acid biosynthesis, a component of the bacterial cell walls. On the basis of the fact that archaea do not have teichoic acid, this suggested the MJ1179 gene product might have a different function. Here we have shown that the MJ1179 gene product is an archaeal FAD synthetase. The MJ1179 gene product is designated as RibL to indicate that it catalyzes the last step of the biosynthesis of FAD in archaea. RibL is present in all methanogens and is distributed with a lower degree of homology among other archaea. Homologues of RibL with a very low degree of homology are present in a few bacteria and are annotated as GCTs. In *Archaeoglobus fulgidus*, the MJ1179 homologue, AF1418, is clustered with riboflavin synthase (*ribC*).

As RibL and GCT are both nucleotidyltransferases, both are expected to catalyze similar reactions (Figure 4). In both cases, a nucleophilic phosphate attacks the α-phosphate of a nucleotide triphosphate, ATP in FAD synthetases and CTP in GCTs. $PP_i$ is released as the other product in both reactions. Of the three conserved GCT sequence motifs (shown in bold in Figure 5), only the HXGH motif is conserved in almost all nucleotidyltransferases, including both the archaeal RibL and the bacterial RibF enzymes (*15*, *16*). The residues in the HXGH motif interact with phosphate groups of nucleotides and stabilize the transition state (*17*).

We have not been able to identify any of the known conserved motifs for FMN and FAD binding (*18*, *19*) in RibL. This indicates that RibL contains a new flavin binding site. The determination of the nature of the flavin binding site must await the X-ray structure of RibL with bound FMN or FAD.

The archaeal RibLs also have a conserved $CX_2HSX_5KEX_5C$ motif in the C-terminus starting at approximately the same location as the conserved RTEGISTT motif in the GCT enzymes (Figure 5). Alkylation of these two cysteines with IAA resulted in inactivation of the protein, indicating the requirement of these cysteine thiols for the activity. Overexpression of either the C126S or C143S RibL mutant in *E. coli* resulted in increased levels of FMN and FAD and reduced levels of riboflavin in the cells, indicating that they had higher activity than the wild type in vivo. The purified C126S mutant also had higher activity than the wild type with $Mg^{2+}$. However, unlike wild-type RibL that has its best

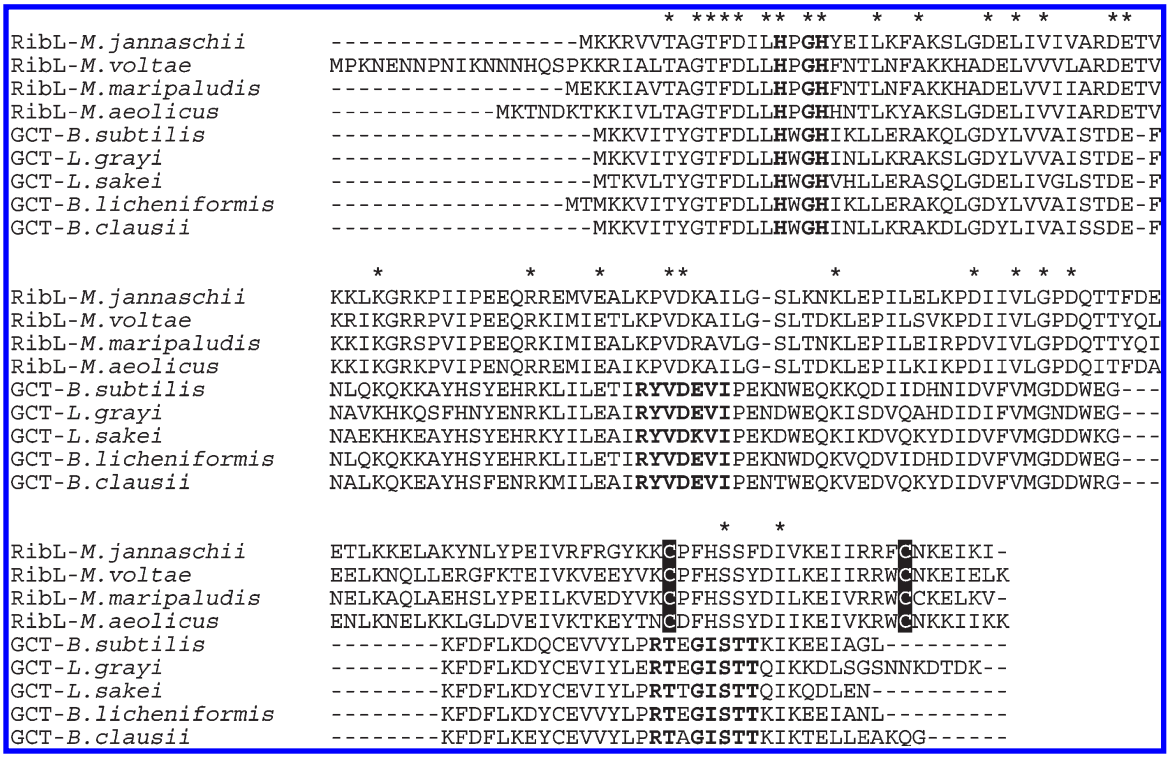


FIGURE 5: Multiple-sequence alignment of RibL and its homologues in other methanogens with some bacterial GCT sequences. The following protein sequences were used to generate this alignment: RibL-*M. jannaschii*, *M. jannaschii*, gi 41018410; RibL-*M. voltae*, *Methanococcus voltae*, gi 163799362; RibL-*M. maripaludis*, *Methanococcus maripaludis*, gi 45358506; RibL-*M. aeolicus*, *Methanococcus aeolicus*, gi 150401726; GCT-*B. subtilis*, *Bacillus subtilis*, gi 16080627; GCT-*L. grayi*, *Listeria grayi*, gi 229556270; GCT-*L. sakei*, *Lactobacillus sakei*, gi 81429187; GCT-*B. licheniformis*, *Bacillus licheniformis*, gi 52787498; GCT-*B. clausii*, *Bacillus clausii*, gi 56964865. Asterisks denote identical residues in both RibL homologues and GCTs. Conserved motifs in GCTs are indicated in bold. The two conserved cysteines in RibL and its homologes are highlighted in black. The alignment was constructed in "The Biology WorkBench" using CLUSTALW.

activity in the presence of $Co^{2+}$, none of the purified mutants exhibited activity with $Co^{2+}$, indicating that $Co^{2+}$ may be binding to the cysteine thiols. Few examples of native enzymes containing bound $Co^{2+}$ are known, and none of these contain two cysteines (*20*−*22*).

We thus see a complex pattern of activation and inactivation of RibL. The enzyme with reduced cysteines, or when one of the two cysteines is replaced with serine, is active. Only when the protein has two reduced cysteines can $Co^{2+}$, $Mn^{2+}$, or $Mg^{2+}$ further activate the enzyme. This could occur by the binding of these metal ions to the cysteines and perhaps the conserved His129. Oxidation or alkylation of the cysteines produces an inactive protein that cannot be reactivated by the addition of metal ions. This indicates that the cysteine thiols may serve as ligands for the metal ions.

Although we do not know the mechanism of enzymatic regulation by the conserved cysteines in RibL, several examples of cysteines being involved in enzyme regulation have been reported. These include cysteines that act as a thiol-based regulatory switch (*23*, *24*) or as a redox sensor (*25*) undergoing oxidation to the disulfide during oxidative stress, reducing enzymatic activity. Alternatively, the conserved cysteines could serve as ligands for metal binding that could be involved in the regulation of the enzyme reaction as seen in the redox-sensing ZAS proteins (*26*).

Most of the known adenylyltransferases, including phosphopantetheine adenylyltransferase (*27*), nicotinate mononucleotide adenylyltransferase (NMAT) (*28*), and FAD synthetase (*2*), catalyze the reverse reaction. Incubation of RibL with FAD and $PP_i$ reveals that RibL does not catalyze the reverse reaction to produce FMN and ATP. Before our work, FAD synthetase from rat liver was the only known example of an irreversible adenylyltransferase (*29*).

One reason why RibL is not able to catalyze the reverse reaction could have been that the enzyme produces two inorganic phosphates rather than $PP_i$. A precedent for this is the MJ0145 gene product, GTP cyclohydrolase III, which was shown to hydrolyze $PP_i$ from GTP followed by hydrolysis of the $PP_i$ into two inorganic phosphates (*30*). That RibL did not hydrolyze the $PP_i$ was confirmed via the establishment that 1 mol of $PP_i$ was formed for each mole of FAD formed. We also observed that $PP_i$ inhibits the forward reaction, which is not seen in other FAD synthetases. However, it has been demonstrated that $PP_i$ also inhibits the activity of GCT from *Bacillus subtilis* (*31*).

RibL also appears to be unique among FAD synthetases in terms of its kinetic reaction mechanism. Hanes plots of [FMN]/*v* versus [FMN] in the presence of different fixed concentrations of ATP showed a series of nonparallel lines not intersecting at a common point, indicating that RibL proceeds by a ternary complex mechanism with substrate (ATP) inhibition (Figure 3). This is opposed to other FAD synthetases that catalyze the reverse reaction, are not inhibited by $PP_i$, and follow an ordered sequential mechanism.

The kinetic constants of RibL (Table 1) are comparable with those of the FAD synthetase in rat liver that shows $K_M^{app}$ values for FMN and ATP of 91 and 71 $\mu$M, respectively (*32*), and quite different from the kinetic properties of FAD synthetase from other organisms, for instance, the reported values ($K_M^{app}$ of FMN, 1 $\mu$M; $K_M^{app}$ of ATP, 37 $\mu$M) for the *Corynebacterium ammoniagenes* enzyme (*2*) and the reported values ($K_M^{app}$ of

FMN, 0.36 $\mu$M; $V_{max}$, 3.9 nmol $min^{-1}$ $mg^{-1}$) for the human enzyme (*33*).

Considering what is now currently known about the differences between the enzymes in the pathways for riboflavin and FAD biosynthesis in the archaea and bacteria (*6*−*8*), the data presented here further support the idea of an independent evolution of the two biosynthetic pathways to FAD in the organisms on earth.

## ACKNOWLEDGMENT

We thank Walter Niehaus for assistance in editing the manuscript, Kim Harich for assistance in obtaining the mass spectral data, and Keith W. Ray for obtaining the MALDI MS data for RibL.

## REFERENCES

1. Manstein, D. J., and Pai, E. F. (1986) Purification and characterization of FAD synthetase from *Brevibacterium ammoniagenes*. *J. Biol. Chem. 261*, 16169–16173.
2. Efimov, I., Kuusk, V., Zhang, X., and McIntire, W. S. (1998) Proposed steady-state kinetic mechanism for *Corynebacterium ammoniagenes* FAD synthetase produced by *Escherichia coli*. *Biochemistry 37*, 9716–9723.
3. Krupa, A., Sandhya, K., Srinivasan, N., and Jonnalagadda, S. (2003) A conserved domain in prokaryotic bifunctional FAD synthetases can potentially catalyze nucleotide transfer. *Trends Biochem. Sci. 28*, 9–12.
4. Frago, S., Velazquez-Campoy, A., and Medina, M. (2009) The Puzzle of Ligand Binding to *Corynebacterium ammoniagenes* FAD Synthetase. *J. Biol. Chem. 284*, 6610–6619.
5. Wu, M., Repetto, B., Glerum, D. M., and Tzagoloff, A. (1995) Cloning and characterization of FAD1, the structural gene for flavin adenine dinucleotide synthetase of *Saccharomyces cerevisiae*. *Mol. Cell. Biol. 15*, 264–271.
6. Mashhadi, Z., Zhang, H., Xu, H., and White, R. H. (2008) Identification and characterization of an archaeon-specific riboflavin kinase. *J. Bacteriol. 190*, 2615–2618.
7. Fischer, M., Romisch, W., Illarionov, B., Eisenreich, W., and Bacher, A. (2005) Structures and reaction mechanisms of riboflavin synthases of eubacterial and archaeal origin. *Biochem. Soc. Trans. 33*, 780–784.
8. Graupner, M., Xu, H., and White, R. H. (2002) The pyrimidine nucleotide reductase step in riboflavin and $F_{420}$ biosynthesis in archaea proceeds by the eukaryotic route to riboflavin. *J. Bacteriol. 184*, 1952–1957.
9. Ammelburg, M., Hartmann, M. D., Djuranovic, S., Alva, V., Koretke, K. K., Martin, J., Sauer, G., Truffault, V., Zeth, K., Lupas, A. N., and Coles, M. (2007) A CTP-dependent archaeal riboflavin kinase forms a bridge in the evolution of cradle-loop barrels. *Structure 15*, 1577–1590.
10. Mukhopadhyay, B., Johnson, E. F., and Wolfe, R. S. (1999) Reactor-scale cultivation of the hyperthermophilic methanarchaeon *Methanococcus jannaschii* to high cell densities. *Appl. Environ. Microbiol. 65*, 5059–5065.
11. Bult, C. J., White, O., Olsen, G. J., Zhou, L., Fleischmann, R. D., Sutton, G. G., Blake, J. A., FitzGerald, L. M., Clayton, R. A., Gocayne, J. D., Kerlavage, A. R., Dougherty, B. A., Tomb, J. F., Adams, M. D., Reich, C. I., Overbeek, R., Kirkness, E. F., Weinstock, K. G., Merrick, J. M., Glodek, A., Scott, J. L., Geoghagen, N. S., and Venter, J. C. (1996) Complete genome sequence of the methanogenic archaeon, *Methanococcus jannaschii*. *Science 273*, 1058–1073.
12. Graham, D. E., Xu, H., and White, R. H. (2002) Identification of coenzyme M biosynthetic phosphosulfolactate synthase: A new family of sulfonate-biosynthesizing enzymes. *J. Biol. Chem. 277*, 13421–13429.
13. Bradford, M. M. (1976) A rapid and sensitive method for the quantitation of microgram quantities of protein utilizing the principle of protein-dye binding. *Anal. Biochem. 72*, 248–254.
14. Deluca, C., and Kaplan, N. O. (1956) Large scale synthesis and purification of flavin adenine dinucleotide. *J. Biol. Chem. 223*, 569–576.
15. Frago, S., Martinez-Julvez, M., Serrano, A., and Medina, M. (2008) Structural analysis of FAD synthetase from *Corynebacterium ammoniagenes*. *BMC Microbiol. 8*, 160.
16. Weber, C. H., Park, Y. S., Sanker, S., Kent, C., and Ludwig, M. L. (1999) A prototypical cytidylyltransferase: CTP:glycerol-3-phosphate cytidylyltransferase from *Bacillus subtilis*. *Structure 7*, 1113–1124.
17. Leatherbarrow, R. J., Fersht, A. R., and Winter, G. (1985) Transition-state stabilization in the mechanism of tyrosyl-tRNA synthetase revealed by protein engineering. *Proc. Natl. Acad. Sci. U.S.A. 82*, 7840–7844.
18. Dym, O., and Eisenberg, D. (2001) Sequence-structure analysis of FAD-containing proteins. *Protein Sci. 10*, 1712–1728.
19. Huerta, C., Borek, D., Machius, M., Grishin, N. V., and Zhang, H. (2009) Structure and mechanism of a eukaryotic FMN adenylyltransferase. *J. Mol. Biol. 389*, 388–400.
20. Nango, E., Kumasaka, T., Hirayama, T., Tanaka, N., and Eguchi, T. (2008) Structure of 2-deoxy-*scyllo*-inosose synthase, a key enzyme in the biosynthesis of 2-deoxystreptamine-containing aminoglycoside antibiotics, in complex with a mechanism-based inhibitor and $NAD^+$. *Proteins 70*, 517–527.
21. Miyanaga, A., Fushinobu, S., Ito, K., and Wakagi, T. (2001) Crystal structure of cobalt-containing nitrile hydratase. *Biochem. Biophys. Res. Commun. 288*, 1169–1174.
22. Arakawa, T., Kawano, Y., Kataoka, S., Katayama, Y., Kamiya, N., Yohda, M., and Odaka, M. (2007) Structure of thiocyanate hydrolase: A new nitrile hydratase family protein with a novel five-coordinate cobalt(III) center. *J. Mol. Biol. 366*, 1497–1509.
23. Paget, M. S., and Buttner, M. J. (2003) Thiol-based regulatory switches. *Annu. Rev. Genet. 37*, 91–121.
24. Hogg, P. J. (2003) Disulfide bonds as switches for protein function. *Trends Biochem. Sci. 28*, 210–214.
25. Zheng, M., Aslund, F., and Storz, G. (1998) Activation of the OxyR transcription factor by reversible disulfide bond formation. *Science 279*, 1718–1721.
26. Zdanowski, K., Doughty, P., Jakimowicz, P., O'Hara, L., Buttner, M. J., Paget, M. S., and Kleanthous, C. (2006) Assignment of the zinc ligands in RsrA, a redox-sensing ZAS protein from *Streptomyces coelicolor*. *Biochemistry 45*, 8294–8300.
27. Miller, J. R., Ohren, J., Sarver, R. W., Mueller, W. T., de Dreu, P., Case, H., and Thanabal, V. (2007) Phosphopantetheine adenylyltransferase from *Escherichia coli*: Investigation of the kinetic mechanism and role in regulation of coenzyme A biosynthesis. *J. Bacteriol. 189*, 8196–8205.
28. Sershon, V. C., Santarsiero, B. D., and Mesecar, A. D. (2009) Kinetic and X-ray structural evidence for negative cooperativity in substrate binding to nicotinate mononucleotide adenylyltransferase (NMAT) from *Bacillus anthracis*. *J. Mol. Biol. 385*, 867–888.
29. Oka, M., and McCormick, D. B. (1987) Complete purification and general characterization of FAD synthetase from rat liver. *J. Biol. Chem. 262*, 7418–7422.
30. Graham, D. E., Xu, H., and White, R. H. (2002) A member of a new class of GTP cyclohydrolases produces formylaminopyrimidine nucleotide monophosphates. *Biochemistry 41*, 15074–15084.
31. Park, Y. S., Sweitzer, T. D., Dixon, J. E., and Kent, C. (1993) Expression, purification, and characterization of CTP:glycerol-3-phosphate cytidylyltransferase from *Bacillus subtilis*. *J. Biol. Chem. 268*, 16648–16654.
32. Yamada, Y., Merrill, A. H., Jr., and McCormick, D. B. (1990) Probable reaction mechanisms of flavokinase and FAD synthetase from rat liver. *Arch. Biochem. Biophys. 278*, 125–130.
33. Galluccio, M., Brizio, C., Torchetti, E. M., Ferranti, P., Gianazza, E., Indiveri, C., and Barile, M. (2007) Over-expression in *Escherichia coli*, purification and characterization of isoform 2 of human FAD synthetase. *Protein Expression Purif. 52*, 175–181.